DYNC1H1 mutations associated with neurological diseases compromise processivity of dynein–dynactin–cargo adaptor complexes

Ha Thi Hoang[a], Max A. Schlager[b,1], Andrew P. Carter[b], and Simon L. Bullock[a,2]

[a]Division of Cell Biology, Medical Research Council (MRC) Laboratory of Molecular Biology, Cambridge CB2 0QH, United Kingdom; and [b]Division of Structural Studies, MRC Laboratory of Molecular Biology, Cambridge CB2 0QH, United Kingdom

Edited by Gary G. Borisy, The Forsyth Institute, Cambridge, MA, and approved January 24, 2017 (received for review December 7, 2016)

Mutations in the human *DYNC1H1* gene are associated with neurological diseases. *DYNC1H1* encodes the heavy chain of cytoplasmic dynein-1, a 1.4-MDa motor complex that traffics organelles, vesicles, and macromolecules toward microtubule minus ends. The effects of the *DYNC1H1* mutations on dynein motility, and consequently their links to neuropathology, are not understood. Here, we address this issue using a recombinant expression system for human dynein coupled to single-molecule resolution in vitro motility assays. We functionally characterize 14 *DYNC1H1* mutations identified in humans diagnosed with malformations in cortical development (MCD) or spinal muscular atrophy with lower extremity predominance (SMALED), as well as three mutations that cause motor and sensory defects in mice. Two of the human mutations, R1962C and H3822P, strongly interfere with dynein's core mechanochemical properties. The remaining mutations selectively compromise the processive mode of dynein movement that is activated by binding to the accessory complex dynactin and the cargo adaptor Bicaudal-D2 (BICD2). Mutations with the strongest effects on dynein motility in vitro are associated with MCD. The vast majority of mutations do not affect binding of dynein to dynactin and BICD2 and are therefore expected to result in linkage of cargos to dynein–dynactin complexes that have defective long-range motility. This observation offers an explanation for the dominant effects of *DYNC1H1* mutations in vivo. Collectively, our results suggest that compromised processivity of cargo–motor assemblies contributes to human neurological disease and provide insight into the influence of different regions of the heavy chain on dynein motility.

dynein | DYNC1H1 | neurological disease | cargo adaptor | processivity

Microtubule motors play a key role in the sorting of many cellular constituents, including organelles, vesicles, aggregated proteins, and macromolecules. Because of their elongated processes, neurons are particularly reliant on a fully operational microtubule-based transport system. This point is underscored by the association of several mutations in microtubule motors and their cofactors with human neurological diseases (1–3). How these mutations affect transport mechanisms is poorly understood. Addressing this issue is expected to provide insight into the cellular basis of neurological disease and also inform diagnostic and therapeutic efforts.

Mutations in the gene encoding the heavy chain of the cytoplasmic dynein-1 (dynein) motor have repeatedly been implicated in neurological diseases (1–13). Dynein is a 1.4-MDa complex that is responsible for the vast majority of cargo transport toward the minus ends of microtubules (14, 15). The complex consists of two copies each of the 530 kDa heavy chain (DYNC1H1), an intermediate chain (either the DYNC1I1 or DYNC1I2 isoform), a light intermediate chain (either the DYNC1LI1 or DYNC1LI2 isoform), and three different light chains [DYNLT1 (Tctex1), DYNLL1 (LC8), and DYNLRB1 (Robl)] (Fig. 1 *A* and *B*). The heavy chain contains a motor domain, which translocates the protein complex toward the minus ends of microtubules using the energy derived from ATP hydrolysis. Key elements within the motor domain include a ring formed by six AAA+ domains, of which AAA1 is the major ATP hydrolysis site, a microtubule-binding domain (MTBD), and an antiparallel coiled-coil stalk that mediates communication between the ring and the MTBD. In addition, there is a buttress domain that emerges from AAA5 of the ring and provides support to the base of the stalk, a linker that is remodeled to produce the powerstroke, and a C-terminal domain that regulates force production and processivity (16). The heavy chain also contains the tail domain, which mediates dimerization and provides a platform for recruiting the other chains. The accessory chains are important for linking the motor to cargos, either through direct interactions or by binding to an intermediary cargo adaptor (17).

At the time of writing, more than 30 heterozygous missense mutations in the *DYNC1H1* gene have been identified in patients diagnosed with spinal muscular atrophy with lower extremity predominance (SMALED) [Online Mendelian Inheritance in Man (OMIM): 158600)] or malformations of cortical development (MCD) (OMIM: 614563) (1–13). SMALED is characterized by muscle weakness in the legs, which is caused by congenital or early childhood-onset loss of spinal cord motor neurons. MCD arises from defective neuronal proliferation or migration during development of the cerebral cortex and is often associated with severe intellectual disability and epilepsy. Whereas some mutations segregate with disease in familial cases (2, 4, 6–8, 13, 18), others have arisen de novo (2, 5, 7, 9–12) (*SI Appendix*, Table S1). For the vast majority of mutations, direct evidence of an effect on dynein function has not been provided, and thus it has not been conclusively shown that they are pathogenic.

Significance

Mutations in microtubule motors and their cofactors are associated with several neurological diseases in humans. How disease-associated mutations affect motor function, and consequently have neuropathological effects, is largely unknown. We take advantage of recent advances in the ability to activate transport of the human dynein complex in vitro to functionally characterize 17 disease-associated mutations in the gene encoding its heavy chain. The vast majority of mutations do not affect the ability of dynein to bind a cargo adaptor but do compromise long-range motion of the motor complex. Our findings suggest that defective motility of cargo–motor complexes contributes to dynein-associated neurological phenotypes and highlight several regions of the enigmatic motor that orchestrate its ability to walk over long distances.

Author contributions: H.T.H., M.A.S., A.P.C., and S.L.B. designed research; H.T.H. and M.A.S. performed research; H.T.H. analyzed data; and H.T.H., A.P.C., and S.L.B. wrote the paper.

The authors declare no conflict of interest.

This article is a PNAS Direct Submission.

Freely available online through the PNAS open access option.

[1]Present address: Roche Diagnostics, 68305 Mannheim, Germany.

[2]To whom correspondence should be addressed. Email: sbullock@mrc-lmb.cam.ac.uk.

This article contains supporting information online at www.pnas.org/lookup/suppl/doi:10.1073/pnas.1620141114/-/DCSupplemental.

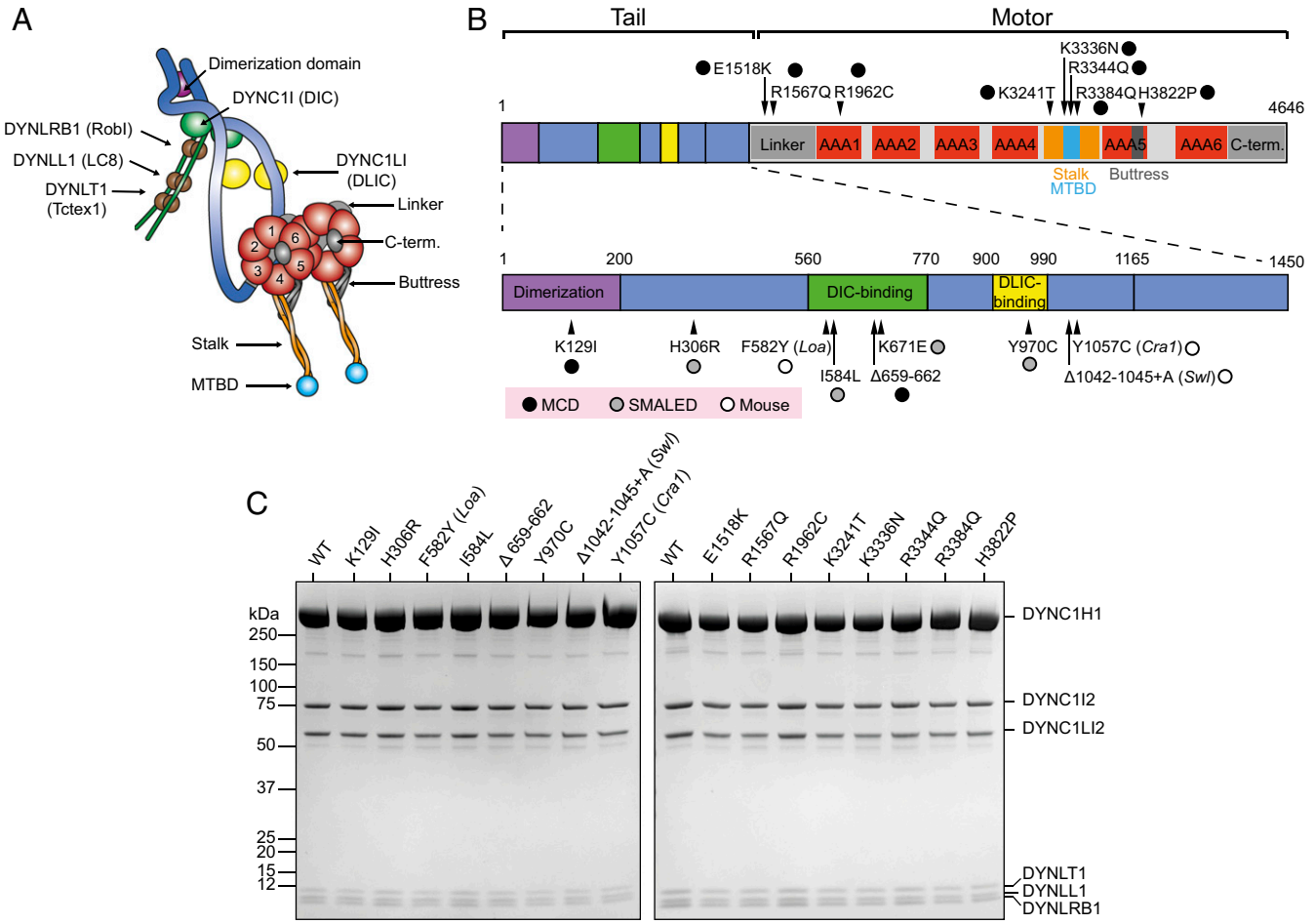

Fig. 1. Positions of DYNC1H1 mutations and accessory chain composition of purified mutant dynein complexes. (*A*) Architecture of the dynein complex. The linker is behind the AAA+ ring in this view. C-term, C-terminal domain. (*B*) Positions in the DYNC1H1 polypeptide of the human and mouse mutations characterized in this study. Mutations discovered in mouse are numbered according to the equivalent residues in human DYNC1H1. H306R has also been associated with Charcot–Marie–Tooth disease type 2O in one pedigree (4). (*C*) Coomassie-stained denaturing gels of human recombinant dynein complexes. The same amount of total protein was loaded per well. None of the DYNC1H1 mutations resulted in an overt change in accessory chain composition of purified dynein complexes compared with the WT. This conclusion was confirmed with dynein samples expressed and purified from an independent construct. K671E DYNC1H1 could not be purified from insect cells in three independent experiments using two different expression constructs.

The links between *DYNC1H1* mutations and neurological disease are further strengthened by the discovery of three mutations that, when heterozygous, cause overlapping neuromuscular and sensory deficits in adult mice (1) (*SI Appendix*, Table S2). The *DYNC1H1* mutant strains were identified in genetic screens due to hind limb clenching and an abnormal gait (1), suggesting parallels with the SMALED phenotype in humans. Heterozygosity for a null mutation in *DYNC1H1* does not cause overt phenotypes in mice (19). This observation, together with the failure to detect nonsense, frameshift, or deletion alleles of *DYNC1H1* in humans with SMALED or MCD, indicates that disease-associated mutations have a dominant-negative or dominant gain-of-function effect. However, with the exception of the mouse *Legs at odd angles* (*Loa*) mutation (20–24), the effects of human and mouse mutations on the motility of the dynein complex have not been investigated in detail.

Here, we assay the effects of 14 *DYNC1H1* patient mutations and the three mouse mutations on the expression and motility of dynein complexes in vitro. These experiments take advantage of two recent advances. First, we exploit a recombinant expression system for the entire human dynein complex (25). This system, which involves the production of the motor complex from a single baculovirus in insect cells, greatly facilitates the purification of dynein complexes with defined mutations. Second, we build on the discovery of a way to study robust minus-end–directed movement of individual dynein complexes in vitro. Whereas individual mammalian dyneins in vitro very rarely exhibit processive behavior (the ability to take repeated steps along microtubules) (25–28), dynein complexes bound to the accessory complex dynactin and a cargo adaptor frequently move processively over very long distances (25, 28–30). Once bound to dynactin and a cargo adaptor, processive movements of dynein are faster and the motor has a greater force output (28, 31).

The best characterized of these activating cargo adaptors is Bicaudal-D2 (BICD2) (17). Studies in rodents have shown that this protein plays an important role in dynein-based cargo transport in neurons (32–34). Consistent with these findings, missense mutations in the human *BICD2* gene are also associated with SMALED (35–37) and cortical malformations (38, 39). The protein uses an N-terminal coiled-coil domain (BICD2N) to bind dynein and dynactin and a C-terminal coiled coil (BICD2C) to bind cargos (17). BICD2's cargos include nuclei that migrate apically in cortical neurons (33, 34, 40) and Golgi-derived vesicles (41). Structural electron microscopy has revealed how BICD2N bridges the interaction between dynein and dynactin (42). The presence of coiled-coil domains in other activating cargo adaptors suggests that they interact with dynein and dynactin through a related mechanism (28–30).

The results of our experiments provide insight into the relationship between *DYNC1H1* mutations and neurological defects. Our finding that all analyzed *DYNC1H1* mutations compromise either dynein expression or motility provides functional evidence for their causative role in disease. We show that the vast majority of mutations inhibit the processive behavior of dynein–dynactin–BICD2N complexes. Mutations with the strongest effects on dynein motility are associated with MCD in humans. Collectively, our results suggest that defective movement of cargo–motor complexes contributes to the neurological phenotypes associated with many *DYNC1H1* mutations. The functional effects of the mutations also reveal that multiple regions of the DYNC1H1 polypeptide regulate processivity of dynein–dynactin–cargo adaptor complexes. Several of these effects cannot be explained by our current understanding of dynein mechanism and thus pave the way for further mechanistic studies.

Results

Expression and Purification of Mutant Dynein Complexes. We focused our study on 17 disease-associated mutations in the *DYNC1H1* gene that were documented at the onset of the project (1) (Fig. 1*B*). This set includes 14 human mutations that are found in individuals diagnosed with MCD or SMALED and the three mouse mutations, *Cramping 1* (*Cra1*), *Loa*, and *Sprawling* (*Swl*). Fifteen of these mutations result in single amino acid substitutions and two (Δ659–662 and *Swl*) produce small deletions in the DYNC1H1 polypeptide (Fig. 1*A*). The affected amino acids are located throughout the tail and motor domains of DYNC1H1 (Fig. 1*B*). More information on the phenotypes associated with these mutations in humans and mice is provided in *SI Appendix*, Tables S1 and S2.

We set out to produce 17 different recombinant human dynein complexes, each containing a unique disease-associated mutation in both copies of DYNC1H1. Mutations were introduced individually by site-directed mutagenesis into a plasmid containing *DYNC1H1* sequences. Mutant *DYNC1H1* genes were then transferred into a plasmid encoding the dynein accessory chains (see *SI Appendix*, *SI Materials and Methods* for details of isoforms used), and the resultant construct transposed into a baculoviral genome (25). A tag introduced on the N terminus of DYNC1H1 allows affinity purification of mutant dynein complexes from baculovirus-infected insect cells and covalent labeling with bright fluorophores (25).

A total of 16 of the 17 mutant dynein complexes could be purified from insect cells by size exclusion chromatography of samples released from the affinity matrix. The exception was the dynein complex containing the K671E mutation, which is located in the region of the tail proposed to associate with the intermediate chain (Fig. 1*B*). In three independent experiments, K671E DYNC1H1 could not be detected during the size exclusion chromatography process, indicating a defect in protein expression or stability.

It has been reported that native dynein complexes isolated from I584L and *Loa* mutant mammalian cells have an altered composition compared with those isolated from wild-type cells (8, 43), although an independent study of native *Loa* dynein found no effect on complex assembly (22). We used our purified protein complexes to determine whether any of the mutations prevent the interaction of DYNC1H1 with one or more of the dynein accessory chains in our expression system. The samples were run on denaturing gels and stained with Coomassie Blue. None of the mutations led to an overt reduction in the amount of the accessory chains copurified with DYNC1H1 (Fig. 1*C*). Collectively, our experiments demonstrate that the vast majority of the DYNC1H1 mutations do not prevent expression of the polypeptide or its association with the other dynein chains. The K671E mutation, however, strongly affects the expression or stability of DYNC1H1.

R1962C and H3822P Strongly Inhibit Microtubule Gliding by Surface-Immobilized Dyneins. We next used a microtubule gliding assay (26, 44) to assess the consequences of the DYNC1H1 mutations on the core mechanical properties of the dynein complex. This involves immobilizing dyneins on a glass surface and incubated them with free microtubules in the presence of ATP (Fig. 2*A*). The collective minus-end–directed activity of dynein translocates microtubules along the surface of the imaging chamber.

Fluorescent microtubules were used in our assays, which can be readily visualized by total internal reflection fluorescence (TIRF) microscopy. In the absence of dynein, microtubules did not adhere to the glass surface (Movie S1). Preadsorption of the glass with wild-type dynein or any of the 16 obtainable mutant complexes resulted in persistent association of microtubules with the surface (e.g., Movie S1). Thus, none of the mutations abolish the microtubule-binding activity of dynein. As expected, wild-type dyneins induced robust gliding of surface-associated microtubules (Fig. 2 *B* and *C* and Movie S1). A total of 14 of the 16 mutant dynein complexes also translocated microtubules robustly, doing so with velocities that were at least as high as those observed for wild-type dynein (Fig. 2*C*).

In contrast, two mutants—R1962C and H3822P, which are in AAA1 and AAA5, respectively—exhibited a very strong defect in microtubule gliding. R1962C dyneins did not produce any movement of microtubules along the glass surface (Fig. 2*B* and Movie S1), whereas 94% of microtubules (117 out of a total of 124 analyzed) were static when H3822P dynein was used (Fig. 2*B* and Movie S1). Those microtubules that were moved by H3822P dynein had a strongly reduced velocity compared to those moved by wild-type dynein [mean ± SEM: H3822P, 30 ± 6 nm/s (n = 7 microtubules); wild-type, 280 ± 15 nm/s (n = 173 microtubules)].

To test the validity of these results, we produced each of the 16 mutant dyneins from an independent baculovirus construct. The strong inhibitory effects of the R1962C and H3822P mutations on microtubule gliding were confirmed when these new protein preparations were used, as was the ability of the other 14 mutations to support robust gliding (*SI Appendix*, Fig. S1). Interestingly, several of the dynein mutations in the tail or linker domains—K129I, F582Y (*Loa*), Δ659–662, Δ1042–1045+A (*Swl*), Y1057C (*Cra1*), E1518K, and R1567C—resulted in a substantial increase in mean microtubule gliding velocity compared with the wild type in both experimental series (Fig. 2*C* and *SI Appendix*, Fig. S1). There was, however, no correlation between the effects of human mutations on microtubule gliding and their association with MCD or SMALED. We conclude from these experiments that the vast majority of dynein mutations do not inhibit motor activity of the human dynein complex in ensemble microtubule gliding assays. R1962C and H3822P, however, strongly inhibit dynein activity in this context.

K129I, K3336N, R3344Q, and R3384Q Compromise the Activation of Processive Dynein Movement. We next investigated the effects of the DYNC1H1 mutations on the processive motion of single, microtubule-associated dynein complexes. As described in the Introduction, processive motion of single mammalian dyneins is rarely observed in the absence of dynactin and a cargo adaptor (25–28). We therefore assayed the motility of the mutant dynein complexes in the presence of both the native dynactin complex, which was purified from pig brain, and recombinant BICD2N (amino acids 1–400) (see *SI Appendix*, Fig. S2 for data on typical purity of these protein samples). To allow visualization of protein complexes, dyneins were labeled with tetramethylrhodamine (TMR) and BICD2N was labeled with Alexa 647 (*SI Appendix*, *SI Materials and Methods*). Wild-type or mutant TMR–dyneins were incubated with dynactin and Alexa 647–BICD2N and protein mixes injected into imaging chambers containing surface-immobilized fluorescent microtubules. TIRF microscopy was then used to capture signals from TMR–dynein and Alexa 647–BICD2N signals on microtubules (Fig. 3*A*).

We first analyzed the TMR signals to assess the behavior of the total population of microtubule-associated dynein complexes. In the presence of dynactin and BICD2N, ∼40% of wild-type dynein complexes that bound to the microtubule underwent processive

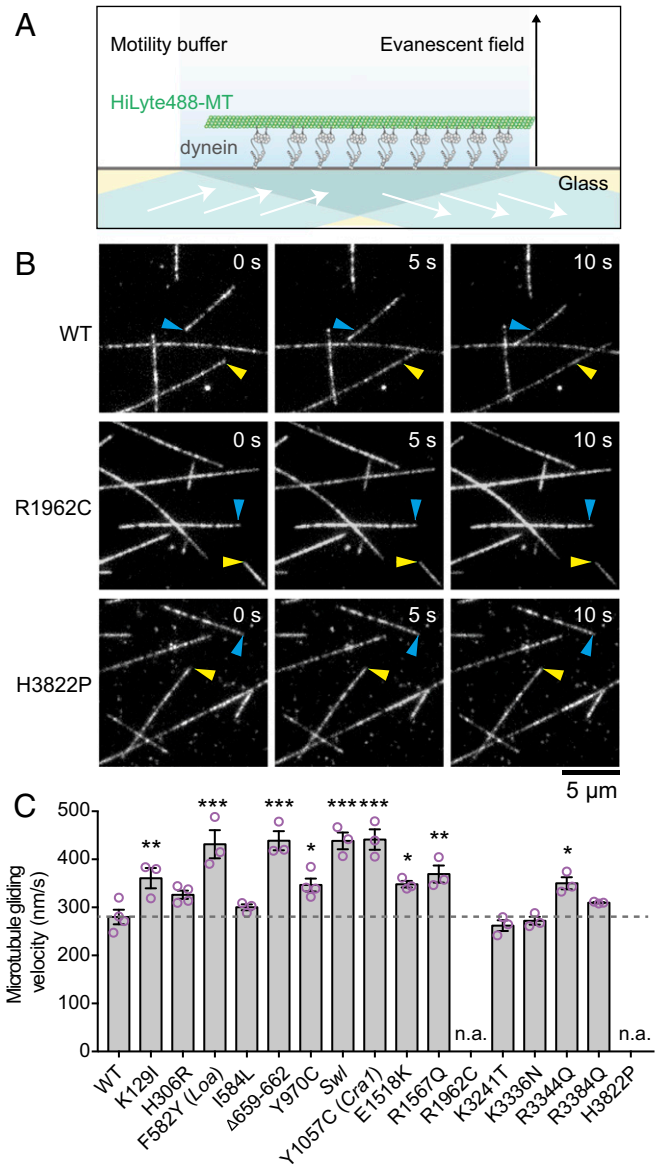

Fig. 2. Effects of DYNC1H1 mutations on microtubule gliding by ensembles of human dynein complexes. (*A*) Diagram of the microtubule gliding assay. Dyneins are absorbed nonspecifically onto the glass surface. MT, microtubule. (*B*) Stills from image series in Movie S1 showing microtubules being translocated by WT dynein but not by dynein containing R1962C or H3822P DYNC1H1. In each condition, the starting position of two microtubule ends are labeled with arrows. (*C*) Quantification of gliding velocities in the presence of WT and mutant dynein complexes. Each magenta circle represents the mean value for an individual chamber (>30 microtubules analyzed per chamber). Gray bars show means of the individual chamber values for each condition; error bars represent SEM. Statistical significance, compared with WT (value illustrated by dashed gray line), was evaluated with a one-way ANOVA with Sidak's multiple comparison test [***$P < 0.001$; **$P < 0.01$; *$P < 0.05$; n.a., not applicable because of the absence (R1962C) or extreme rarity (H3822P) of microtubule gliding].

movement (Fig. 3 *B* and *C*). Less than 3% of the wild-type dyneins exhibited processive motion when dynactin and BICD2N were omitted (Fig. 3*C*). These values were similar to those observed in our previous study of wild-type dynein in the presence and absence of dynactin and BICD2N (25).

As expected from their effects on microtubule gliding by dynein, the R1962C and H3822P mutations strongly inhibited processive motion of single, microtubule-associated dynein complexes in the presence of dynactin and BICD2N (Fig. 3 *B* and *C*). No processive complexes were observed for R1962C dynein (Fig. 3*C*), whereas only 5% of microtubule-associated H3822P complexes exhibited processive movement (Fig. 3*C*). Thus, although both R1962C and H3822P mutations had very strong effects on the behavior of single dynein complexes in the presence of dynactin and BICD2N, only the R1962C mutation completely abolished motility. Four other DYNC1H1 mutations—K129I, K3336N, R3344Q, and R3384Q—resulted in only 10–25% of microtubule-associated TMR–dynein complexes undergoing processive motion in the presence of dynactin and BICD2N, which equates to an approximately two- to fourfold reduction compared with the wild type (Fig. 3 *B* and *C*). K129I is in the N-terminal region of the DYNC1H1 tail and K3336N, R3344Q, and R3384Q are in the MTBD (Fig. 1*B*). The tail mutation I584L resulted in a smaller, but statistically significant, reduction in the frequency of processive motion of microtubule-associated dyneins in the presence of dynactin and BICD2N compared with the wild type (Fig. 3*C*). The remaining mutations had no effect on the frequency of processive motion (Fig. 3*C*). We confirmed that the K129I, R1962C, K3336N, R3344Q, R3384Q, and H3822P mutations reduced the frequency of processive movements in another experimental series, which used independent preparations of the 16 mutant dynein complexes, dynactin, and BICD2N (*SI Appendix*, Fig. S3 *A* and *B*). However, the subtle effect of the I584L mutation observed previously was not reproduced in this series (*SI Appendix*, Fig. S3*B*).

In summary, these experiments demonstrate that several DYNC1H1 mutations reduce the incidence of processive behavior of microtubule-associated dynein complexes that is induced by dynactin and BICD2N. The strongest effects were observed for R1962C and H3822P, which is consistent with the strong inhibitory effects of these mutations on microtubule gliding. K129I, K3336N, R3344Q, and R3384Q, which did not compromise dynein activity in the gliding assay, consistently led to a strong reduction in the incidence of processive movement of dynein complexes.

Most DYNC1H1 Mutations Do Not Inhibit Binding of Dynein to Dynactin and BICD2N. We next investigated how certain DYNC1H1 mutations reduce the incidence of processive movement of microtubule-associated dyneins. This could be caused by reduced association of dynein with dynactin and BICD2N, or by compromised motility of dynein–dynactin–BICD2N complexes once they are assembled. To distinguish between these possibilities, we determined the percentage of microtubule-associated dynein complexes containing each DYNC1H1 mutation that associated with dynactin and BICD2N. The Alexa 647–BICD2N signals were overlayed on the TMR–dynein signals (Fig. 4*A* and *SI Appendix*, Figs. S4 and S5) and colocalization scored. As BICD2N can only bind dynein in the presence of dynactin (25, 28, 45), dual colored puncta must represent dynein–dynactin–BICD2N complexes. Consistent with this notion, whereas ~75% of the total population of wild-type TMR–dyneins on microtubules had an Alexa 647–BICD2N signal when dynactin was included in the assay (Fig. 4*B*), no colocalization was observed when dynactin was excluded (*SI Appendix*, Fig. S6). As expected, in the presence of dynactin, almost all processive wild-type dynein complexes had a detectable signal from BICD2N (Fig. 4*A* and *SI Appendix*, Fig. S4). However, many wild-type dyneins with a BICD2N signal did not move processively (Fig. 4 *A* and *C*), in agreement with previous observations that not all dynein–dynactin–BICD2N complexes are active (25, 28).

Our analysis for mutant complexes revealed that only two DYNC1H1 mutations—K3241T and K3336N—significantly reduced the degree of colocalization of dynein and BICD2N on microtubules (Fig. 4*B*). The magnitude of these effects was, however, rather small: ~60% of K3241T dyneins colocalized with BICD2N, with this value decreasing to 50% for K3336N (Fig. 4*B*).

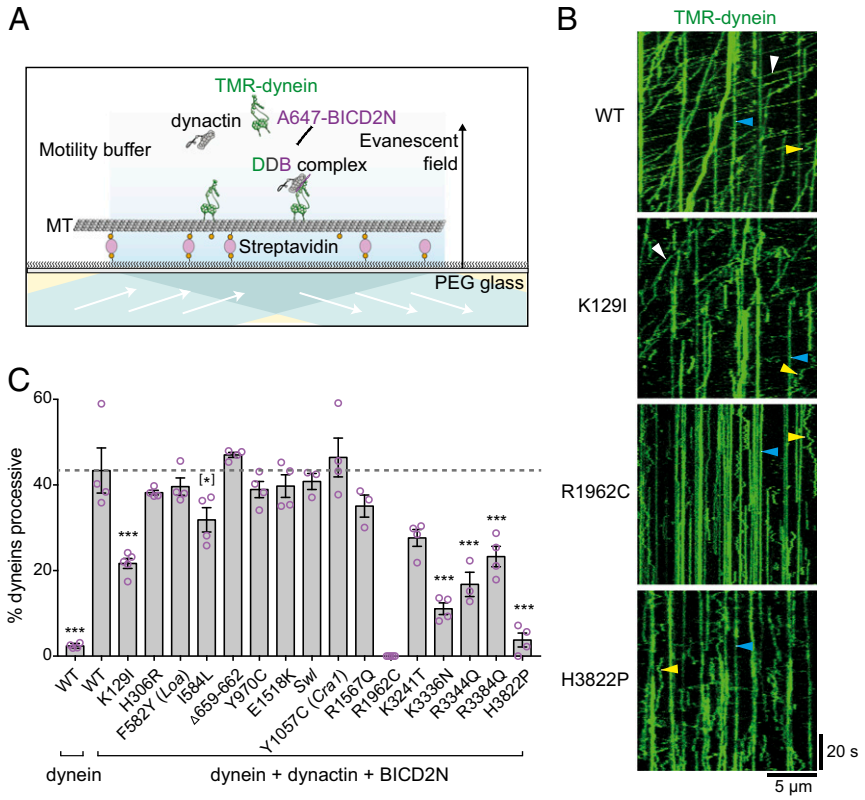

Fig. 3. Effects of DYNC1H1 mutations on processive movement of individual dynein complexes in the presence of dynactin and BICD2N. (*A*) Diagram of the assay for processive movement of dynein. Microtubules (MTs) are immobilized on biotin (orange)/streptavidin (pink)-coated glass using biotin present on a fraction of tubulins. (*B*) Kymographs (time–distance plots) showing examples of the effect of DYNC1H1 mutations on processive movement of dynein (green) in the presence of dynactin and BICD2N. White, yellow, and blue arrowheads indicate examples of processive, diffusive, and static behavior, respectively. (*C*) Quantification of effects of DYNC1H1 mutations on percentage of microtubule-associated dyneins that move processively in the presence of dynactin and BICD2N. Each magenta circle represents the mean value for an individual chamber (>70 dynein complexes analyzed per chamber). Throughout the study, each chamber used an independent assembly mix of dynein, dynactin, and BICD2N. Gray bars show means of the individual chamber values for each condition; error bars represent SEM. Statistical significance, compared with WT dynein in the presence of dynactin and BICD2N (value illustrated by dashed gray line), was evaluated with a one-way ANOVA with Sidak's multiple comparison test (***$P < 0.001$; *$P < 0.05$; [*]$P < 0.05$ but a significant difference was not reproduced in a second experimental series (*SI Appendix*, Fig. S3).

We conclude that the majority of dynein mutations do not alter the ability of dynein to associate with dynactin and BICD2N in vitro.

These data revealed that the K129I, R1962C, R3344Q, R3384Q, and H3822P mutations do not inhibit the processive motion of dynein by interfering with dynein's association with dynactin and BICD2N, but rather by compromising the motility of dynein–dynactin–BICD2N complexes. The effect of these mutations on the ability of dynein–dynactin–BICD2N complexes to initiate processive movement was confirmed directly by analyzing the motility of those TMR–dyneins with an Alexa 647–BICD2N signal (Fig. 4*C*). Interestingly, the mutation that exhibited the strongest reduction in the colocalization of dynein and BICD2N—K3336N—also significantly reduced the frequency of processive motion of those dynein–dynactin–BICD2N complexes that were formed (Fig. 4*C*).

Nonprocessive dynein complexes can be statically bound to microtubules or undergo short-range diffusion along the lattice (25–28). This latter behavior is likely to reflect a weak interaction of the motor complex with the microtubule (27). The reduction in processive motion of dynein–dynactin–BICD2N complexes containing the K129I, K3336N, R3344Q, and R3384Q mutations was accompanied by a significant increase in the frequency of diffusive behavior (Fig. 4 *C*–*E*). In contrast, the vast majority of the dynein–dynactin–BICD2N complexes containing the R1962C mutation in AAA1 exhibited static binding to microtubules (Fig. 4 *C*–*E* and *SI Appendix*, Fig. S3*A*). The H3822P mutation increased the incidence of both static and diffusive events (Fig. 4 *C*–*E*). Collectively, these data indicate that several DYNC1H1 mutations affect the probability of processive, diffusive, and static behavior of dynein–dynactin–BICD2N complexes on microtubules.

The Vast Majority of Dynein Mutations Reduce the Run Length of Processive Dynein–Dynactin–BICD2N Complexes. We next examined the effects of the DYNC1H1 mutations on the run length and velocity of those dynein–dynactin–BICD2N complexes that exhibited processive motion. R1962C dyneins were excluded from this analysis as they displayed no processive movements. Because processive movements were very rare for H3822P dyneins, we had to pool run length and velocity values across chambers for this mutant (*SI Appendix*, Fig. S7) rather than performing chamber-by-chamber analysis.

Operationally, run length was defined as the distance a processive complex traveled before pausing or detaching from the microtubule. Strikingly, all 15 mutations analyzed resulted in an approximate twofold reduction in the mean run length of dynein–dynactin–BICD2N complexes (Fig. 5*A* and *SI Appendix*, Figs. S7 and S8 *A* and *C*). The ability of DYNC1H1 mutations to reduce run lengths was confirmed by analysis of the in vitro motility assays that were performed with independent preparations of dynein complexes, dynactin, and BICD2N (*SI Appendix*, Fig. S9 *A*–*C*). Thus, all DYNC1H1 disease mutations analyzed decrease the travel distance of processive dynein–dynactin–BICD2N complexes.

We then analyzed the effects of the mutations on the velocity of processive dynein–dynactin–BICD2N complexes. The K3336N, R3344Q, R3384Q, and H3822P mutations caused an approximately twofold decrease in mean velocity of dynein–dynactin–BICD2N complexes (Fig. 5*B* and *SI Appendix*, Figs. S7, S8 *B* and *D*, and S9 *D* and *E*). These mutations also consistently reduced the frequency of processive transport events by dynein–dynactin–BICD2N complexes (Fig. 3*C*). Thus, K3336N, R3344Q, R3384Q, and H3822P affect multiple aspects of dynein motility. The other 11 mutations analyzed did not consistently affect the velocity of processive dynein–dynactin–BICD2N complexes (Fig. 5*B* and *SI Appendix*, Fig. S9*D*). Thus, the ability of several tail and linker mutations to increase the velocity of microtubule gliding by teams of immobilized dyneins were not accompanied by an increase in the speed at which dynein–dynactin–BICD2N complexes run along microtubules. Our finding that the *Loa* mutation reduces run lengths but not velocities of a dynein–dynactin–cargo adaptor complex are consistent with results of high spatiotemporal imaging of lysosomes in *Loa* mutant mouse axons (22).

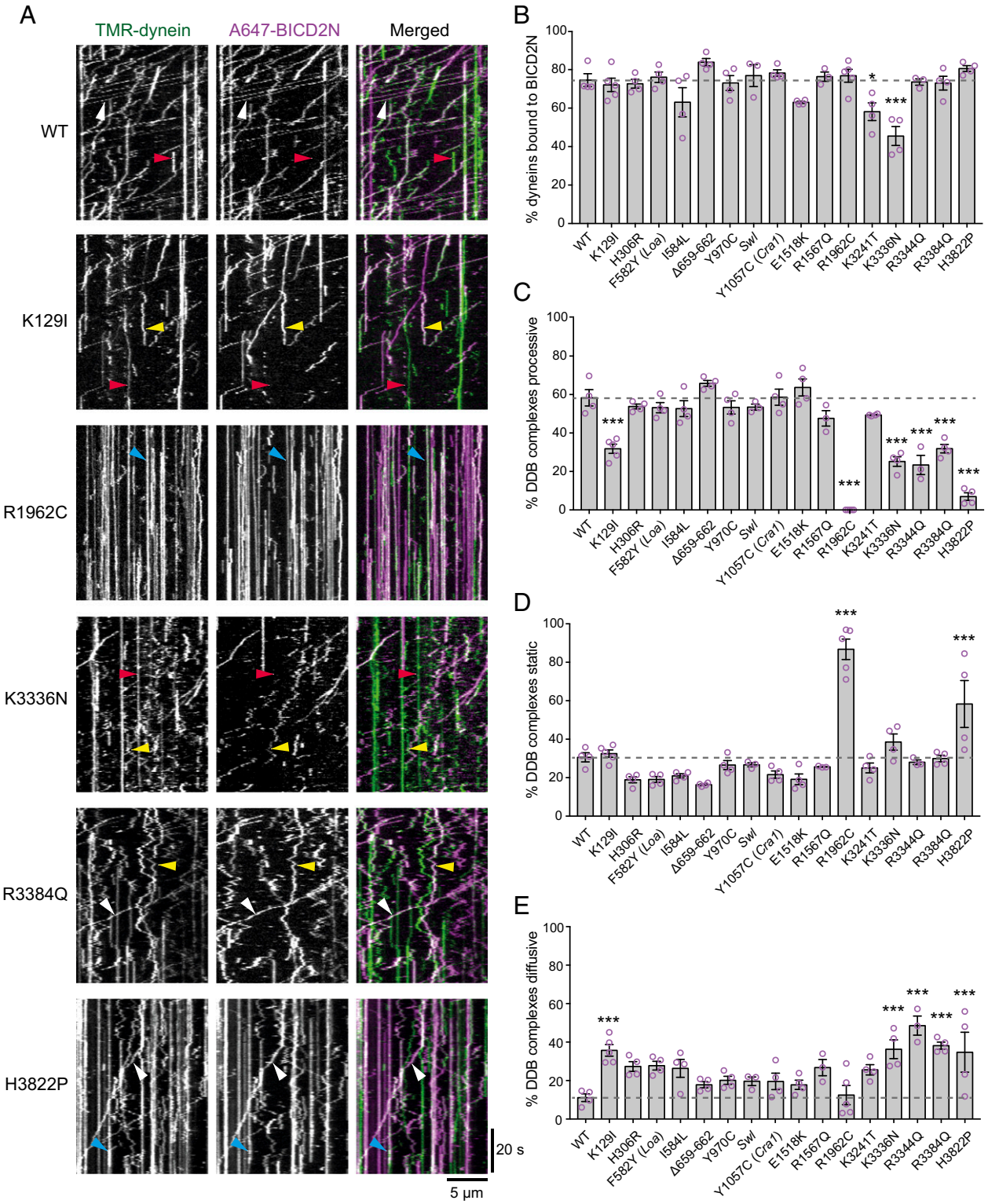

Fig. 4. Effects of DYNC1H1 mutations on the assembly and processivity of dynein–dynactin–BICD2N complexes. (*A*) Kymographs showing examples of frequent colocalization of mutant TMR–dynein complexes (green in merged images) with Alexa 647–BICD2N (magenta in merged images) on microtubules in the presence of dynactin (see *SI Appendix*, Figs. S4 and S5 for examples of other mutant complexes). Colocalization indicates formation of a dynein–dynactin–BICD2N complex. White, blue, and yellow arrowheads indicate examples of colocalization of Alexa 647–BICD2N with TMR–dynein exhibiting processive, static, and diffusive behavior, respectively. Red arrowheads indicate examples of TMR–dynein complexes without an Alexa 647–BICD2N signal. (*B*) Quantification of the percentage of all microtubule-associated dyneins that, in the presence of dynactin, colocalizes with BICD2N. (*C–E*) Quantification of the percentage of microtubule-associated dynein–dynactin–BICD2N (DDB) complexes that exhibits processive (*C*), static (*D*), and diffusive (*E*) behavior. In *B–E*, each magenta circle represents the mean value for an individual chamber [>70 dynein complexes (*B*) or 50 dynein–dynactin–BICD2N (*C–E*) complexes analyzed per chamber]. Gray bars show means of the individual chamber values for each condition; error bars represent SEM. Statistical significance, compared with WT (value illustrated by dashed gray line), was evaluated with a one-way ANOVA with Sidak's multiple comparison test (***$P < 0.001$; *$P < 0.05$).

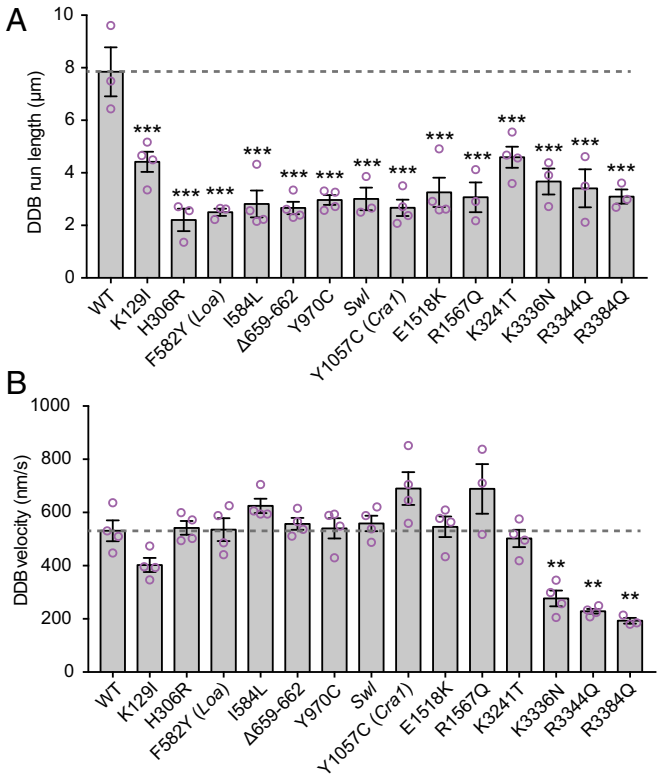

Fig. 5. Effects of DYNC1H1 mutations on the run length (*A*) and velocity (*B*) of processive dynein–dynactin–BICD2N complexes. Each magenta circle represents the mean value for an individual chamber (>50 runs or velocity segments were analyzed per chamber). Gray bars show means of the individual chamber values for each condition; error bars represent SEM. Statistical significance, compared with WT (values illustrated by dashed gray line), was evaluated with a one-way ANOVA with Sidak's multiple comparison test (***$P < 0.001$; **$P < 0.01$). See *SI Appendix*, Fig. S8 for data on run length and velocity distributions.

Overall, we conclude from our analyzes that the vast majority of disease-associated DYNC1H1 mutations impair dynein function not by inhibiting binding to processivity activators, but rather through restriction of movement of the intact transport complex.

Discussion

We have used a recently developed insect cell expression system and in vitro motility assays to characterize the effects on dynein motility of a large series of mutations in DYNC1H1 that are associated with neurological disease in human and mouse. Our results are summarized in Fig. 6. We identify two mutations—R1962C and H3822P—that severely compromise the core mechanochemical properties of human dynein as judged by their strong effects on microtubule gliding by ensembles of dyneins, as well as on processive movement of individual motor complexes in the presence of dynactin and BICD2N. Four mutations—K129I, K3336N, R3344Q, and R3384Q—do not inhibit microtubule gliding by ensembles of human dynein but consistently reduce the frequency of processive movement of individual, microtubule-associated dyneins in the presence of dynactin and BICD2N. These mutations also strongly reduce the travel distance of processive events, with K3336N, R3344Q, and R3384Q additionally leading to a significant slowing of these movements. A further 10 mutations, including all 3 that were discovered in the mouse, had a more restricted effect on the behavior of human dynein in our assays. The predominant effect of these mutations was a substantial decrease in the length of processive transport events in the presence of dynactin and BICD2N. Overall, the mutations studied had little effect on the ability of dynein to associate with dynactin and BICD2N, suggesting that they result in BICD2's cargos being linked to dynein complexes with defective motility.

Mechanistic Effects of DYNC1H1 Mutations. Although structural and single molecule studies have provided remarkable insights into dynein mechanism, the dynamic changes within the motor complex that generate movement of cargos along microtubules are only partially understood. Our analysis of disease-associated mutations highlight several positions of the ∼4,600 amino-acid-long DYNC1H1 that are important for efficient motility of a dynein–dynactin–cargo adaptor complex.

Eight of the mutations we studied are located in the motor domain (Fig. 7*A*). A high-resolution structure of the motor domain of mammalian DYNC1H1 has not been reported. However, homology modeling of the motor domain based on atomic structures from other dyneins (46, 47) or a pseudoatomic model of the MTBD from mouse DYNC1H1 (48) offer an explanation for how several of the mutations affect motor function. The R1962C mutation is located within the large domain of AAA1 (AAA1L) and so affects the main ATPase site in dynein. In the presence of ADP, there is a cleft between AAA1 and AAA2 and R1962 points into solution (Fig. 7*B*). Upon ATP binding and hydrolysis, the cleft closes and R1962 becomes part of a network of contacts between AAA1L and AAA2L (Fig. 7*C*). The R1962C mutation would disrupt these contacts and is thus expected to destabilize the conformation dynein enters during ATP hydrolysis. Destabilization of this state would account for the lack of R1962C dynein activity in the microtubule gliding assay, as well as in the context of individual

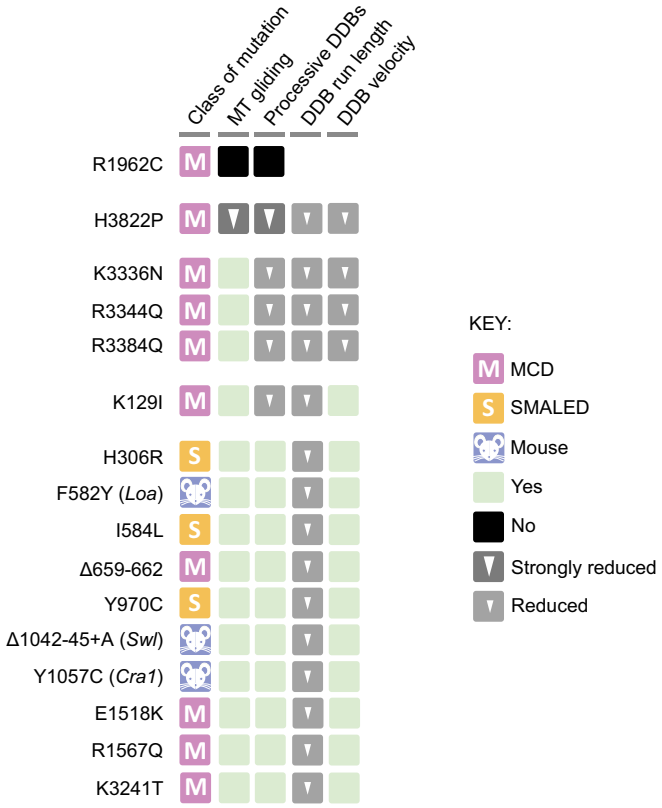

Fig. 6. Summary of the consequences of DYNC1H1 mutations on dynein motility. Mutations are clustered based on similarities of their effects on purified dynein complexes, with the severity of each cluster decreasing from *Top* to *Bottom*. Within each cluster, mutations are ordered in an N–C-terminal direction. MT, microtubule; DDB, dynein–dynactin–BICD2N. Note that K671E DYNC1H1 could not be purified.

dynein–dynactin–BICD2N complexes. Because closure of AAA1 and AAA2 also plays a key role in the structural rearrangements that lower the affinity of the MTBD for the microtubule (49), an inhibitory effect on this process could also explain why most R1962C dyneins are stably bound to a single site on the microtubule rather than engaged in lattice diffusion.

H3822P has a similar affect to R1962C in the in vitro motility assays, with very little microtubule gliding activity or processive movement of dynein–dynactin–BICD2N complexes. H3822 is in the small domain of AAA5 (AAA5S) close to the interface with the large domain of AAA6 (AAA6L) (Fig. 7*D*). AAA6L and AAA5S move together as a block during the ATP hydrolysis cycle (49). AAA5L also contains the buttress (Fig. 7*A*), which couples these movements to changes in the conformation of the stalk and the affinity of the MTBD for microtubules. H3822P would disrupt a cluster of AAA5S residues (F3823, L3824, and Y3825) at the interface with AAA6L (Fig. 7*D*). This mutation may therefore compromise dynein motility by interfering with the communication pathway that couples rearrangements in the AAA+ ring to changes in the MTBD.

As noted previously (2), three of the mutations we analyzed—K3336N, R3344Q, and R3384Q—lie at the interface between the MTBD and microtubules (Fig. 7 *A* and *E*) (48). All three mutations strongly reduce the frequency, travel distance, and velocity of processive movements of individual, microtubule-associated dynein–dynactin–BICD2N complexes but have no effect on microtubule gliding by surface-immobilized dyneins. We found that these mutations significantly increase the frequency of diffusion of dynein–dynactin–BICD2N complexes (Fig. 4*E*), suggesting that they weaken the interaction between the MTBD and the microtubule. Consistent with this notion, K3336N and R3384Q reduce the sedimentation of the MTBD with microtubules in the context of a fusion protein with a heterologous coiled-coil domain (2). By interfering with the tight binding state of the MTBD, the K3336N, R3344Q, and R3384Q mutations may disrupt the ability of the dynein heads to make repeated steps. This behavior is essential for processive movement of individual complexes but is unlikely to be required for microtubule gliding by teams of surface-immobilized motors (26).

The three other disease-associated mutations in the motor domain—E1518K, R1567Q, and H3241T—affect surface exposed residues. E1518K and R1567Q are located in the linker domain (Fig. 7*F*), whereas K3241 is found within the stalk (Fig. 7*G*). These mutations reduce the run length of dynein–dynactin–BICD2N complexes but do not significantly affect the frequency or velocity of processive movements. How these three mutations affect travel distance of dynein–dynactin–BICD2N complexes is currently not clear, but they could conceivably modulate the dynamic conformational changes exhibited by the linker and stalk during the ATPase cycle.

The remaining DYNC1H1 mutations we studied are in the tail domain, for which there is no high-resolution structural information. We anticipated that at least some of the mutations in the DYNC1H1 tail would affect dynein function by altering the interaction with the dynein accessory chains, dynactin or BICD2N. Our failure to detect changes in the ability of the mutant DYNC1H1 proteins to interact with these factors was therefore surprising. These mutations do, however, compromise processive movements of microtubule-associated dynein–dynactin–BICD2N complexes (Fig. 6).

There are precedents for mutations in the tail of DYNC1H1 having effects on the motor domain without affecting interactions with binding partners. Dyneins isolated from mice heterozygous for the *Loa* mutation have curtailed minus-end–directed motion in vitro and evidence of disrupted coordination between motor heads, despite having a full complement of accessory chains (22). Because the study was performed in the absence of processivity activators, it is, however, unclear how the findings relate to our observations of the effect of this mutation on dynein–dynactin–BICD2N complexes. It has also be demonstrated that a mutation in the tail of DYNC1H1 in the filamentous fungus *Aspergillus nidulans* (in a residue equivalent to position 186 of the human protein) reduces the frequency and velocity of minus-end–directed cargo transport in vivo without affecting the composition of the dynein complex or its association with dynactin (50). Our study reveals that the ability of the tail to regulate the behavior of the motor domain is not just restricted to the regions containing the *Loa* and *Aspergillus* mutations. We show that many sites along the DYNC1H1 tail are involved in regulating motor activity in the context of a defined dynein–dynactin–cargo adaptor complex. Our data also suggest that disruption of this regulation contributes to

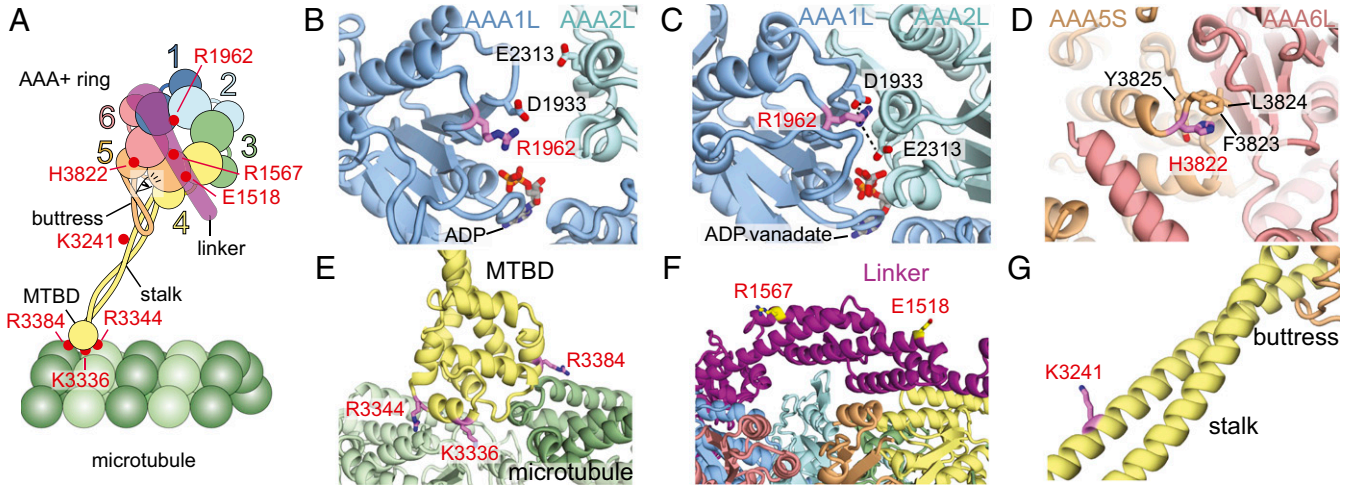

Fig. 7. Structural analysis of mutated residues in the DYNC1H1 motor domain. (*A*) Cartoon of a microtubule-bound dynein motor domain, showing positions of DYNC1H1 mutations (red circles). Individual AAA+ domains, which are divided into large and small subdomains, are labeled with a colored number. MTBD, microtubule binding domain. Eye shows the viewpoint for *F*. (*B*–*F*) Structural analysis of the positions of mutated residues in the DYNC1H1 motor domain. Domains are colored as in *A*; side chains of mutated residues are shown in magenta in *B*–*E* and *G*, and yellow in *F*. See text for details. Homology models are based on the structures of the motor domain of *Dictyostelium* dynein-1 bound to ADP [Protein Data Bank (PDB): 3VKG] (*B*, *D*, *F*, and *G*), human cytoplasmic dynein-2 bound to ADP.vanadate (PDB:4RH7) (*C*), and a pseudoatomic model from a 9-Å cryo-EM structure of the MTBD of mouse DYNC1H1 bound to microtubules (PDB: 3J1T) (*E*). ADP.vanadate is a nucleotide analog that mimics the transition state of ATP hydrolysis.

neurological diseases in humans. Remarkably, the tail mutation with the strongest effect on processive movements of the dynein–dynactin–BICD2N complex in our study—K129I—is the one farthest away from the motor domain. Although this mutation is found within the so-called "dimerization domain" (42), it does not disrupt the ability of the heavy chains to dimerize (*SI Appendix*, Fig. S10) and thus compromises the activity of the motor domain in the context of the full dynein–dynactin–BICD2N complex. Our identification of a large number of mutations in the tail that affect processive movements of dynein–dynactin–cargo adaptor complexes will aid future efforts to understand the basis of the communication between the tail and motor domains. This work may also illuminate how some mutations in the tail increase the velocity of microtubule gliding by teams of isolated dyneins.

Insights into the Basis of DYNC1H1-Associated Neurological Diseases. Many of the *DYNC1H1* mutations identified in patients have either arisen de novo or have been identified in small families where segregation studies cannot conclusively demonstrate pathogenicity. In these cases, the evidence for involvement in disease has also included the evolutionary conservation of the mutated residue and differences in the physicochemical properties of the substituted amino acid. However, functional assays are highly desirable when ascribing causality to rare sequence variants (51). We find that all 14 human *DYNC1H1* mutations tested, including several de novo mutations (*SI Appendix*, Table S1), compromise the expression or motility of the dynein complex in vitro. These data provide functional evidence for their contribution to neurological disease. Interestingly, of the 16 human or mouse mutations that support production of the recombinant dynein complex, the 6 with the strongest effects on dynein motility are associated with MCD in humans (Fig. 6). All three SMALED mutations that could be assayed in the context of the purified motor complex fell into the class with the weakest effects (Fig. 6). These mutations are among the group that only compromised run lengths of processive dynein–dynactin–BICD2N complexes. These findings raise the possibility that MCD and SMALED are caused by different degrees of inhibition of dynein motility, rather than inactivation of distinct dynein-related processes. Consistent with the notion that dynein-associated neurological diseases are on the same spectrum, at least some individuals with *DYNC1H1* mutations have combined defects in cortical development and spinal motor neurons (2, 4, 7, 8, 10). For example, some of the DYNC1H1 mutations we studied were found in individuals with both MCD and foot deformities consistent with axonal neuropathy (2) (*SI Appendix*, Table S1). Other mutations were identified in SMALED patients noted to also have mild intellectual disability (4, 8) (*SI Appendix*, Table S1).

However, four de novo MCD-associated mutations—Δ659–662, E1518K, R1567Q, and K3241T—fell into the class that only exhibited reduced run lengths of dynein–dynactin–BICD2N complexes. The overt cortical development defects in the individuals with these mutations may therefore result from an interaction with other mutations present in their genomes or environmental factors. The notion that extrinsic factors influence the phenotypes associated with human DYNC1H1 mutations is supported by the observation that the H306R variant gives rise to different symptoms in different pedigrees (4, 6) (*SI Appendix*, Table S1). Alternatively, by impacting on interactions of DYNC1H1 with other binding partners, Δ659–662, E1518K, R1567Q, and K3241T may exert stronger effects on dynein motility in vivo than were evident in our study.

A key finding of our work is that the vast majority of DYNC1H1 mutations do not inhibit the ability of dynein to associate with dynactin and BICD2N, but do compromise the motile properties of dynein–dynactin–BICD2N complexes. An ability of dyneins with compromised motility to bind BICD2, and potentially other cargo adaptors, offers a possible explanation for the dominant effects of *DYNC1H1* mutations in vivo. The mutant dyneins would be expected to provide a link between cargos and microtubules. However, processive movements of these cargos would be shorter, slower, or less frequent, thus compromising cargo delivery within neurons. Provided levels of DYNC1H1 protein are not limiting, heterozygosity for a null mutation in *DYNC1H1* would not be expected to have the same effect. This hypothesis can explain why mice that are heterozygous for a *DYNC1H1* null allele are asymptomatic, and frameshift, nonsense, and deletion alleles have not been recovered in humans with MCD or SMALED.

As noted previously (22), neurons with long axonal processes are likely to be particularly sensitive to reduced processivity of cargo–dynein complexes. This sensitivity could account for the association of those *DYNC1H1* mutations that have relatively mild effects on dynein activity in vitro with SMALED, which predominantly affects spinal motor neurons in the legs. Mutations with stronger effects on dynein motility may additionally compromise cargo delivery in neurons with shorter processes, such as those in the developing cortex, which could contribute to MCD. This hypothesis is seemingly challenged by the observation that some patients with MCD were not diagnosed with SMALED-like features (2). However, it is conceivable that variation in genetic background and environmental factors influences how alterations in cargo transport are manifested at the phenotypic level in patients. In the future, it will be important to use isogenic animal models to evaluate how mutations found in individuals with MCD and SMALED affect cargo transport in different neuronal cell types.

Not all DYNC1H1 mutations studied could have their functional effects ascribed to reduced motility of the dynein complex. We found one mutation—K671E—that consistently prevented the purification of DYNC1H1 from insect cells. This mutation is found within the region of the tail that associates with dynein's intermediate chain. Depletion of the intermediate chain in cells causes a large reduction in the level of DYNC1H1 (52), indicating that stability of the heavy chain is dependent on its ability to associate with the intermediate chain. Any ability of the K671E mutation to disrupt intermediate chain binding would therefore be expected to destabilize DYNC1H1. It is not clear why heterozygosity for this mutation is associated with a phenotype in humans—SMALED (8)—whereas heterozygosity for nonsense, frameshift, or deletion alleles in *DYNC1H1* is not. However, because defects in protein homeostasis have frequently been linked to neurological diseases (53), it is tempting to speculate that the destabilizing effect of the K671E mutation results in a misfolded or aggregrated intermediate that has a pathological effect in neurons.

Perspective. Since this study was initiated, the number of *DYNC1H1* mutations that have been associated with human neurological disease has risen substantially. For example, *DYNC1H1* variants of unknown clinical significance were commonly found in patients undergoing genetic screening for peripheral neuropathy (54). The number of variants identified in this gene is set to increase further with the adoption of next-generation sequencing in routine clinical practice. Our work describes a pipeline that can be used to evaluate whether and how newly discovered mutations affect dynein function. The same strategy can also be used to study the functional effects of *BICD2* variants identified in patients.

Posttranslational modifications of tubulin exhibit distinct subcellular localizations in neurons (55) and are emerging as important regulators of mammalian dynein–dynactin function (56). It will therefore also be interesting to explore how disease-associated mutations affect the interactions of dynein–dynactin–cargo adaptor complexes with microtubules containing defined posttranslational modifications. We anticipate that studying the effects of disease-associated variants in vitro will also help clarify how the dynein machinery operates in a nonpathological setting. Ultimately, in vitro studies of mutations, coupled to analysis in cellular systems, should inform therapeutic efforts to tackle dynein-associated neurological diseases.

Materials and Methods

Protein production and labeling, in vitro motility assays, and quantification were performed as described (25). Full methods are provided in *SI Appendix, SI Materials and Methods*.

ACKNOWLEDGMENTS. We thank all members of the S.L.B. and A.P.C. laboratories, and in particular J. Baumbach, C. Dix, H. Foster, H. Schmidt, and L. Urnavicius, for assistance and advice; and A. Rossor (University College London Institute of Neurology), M. McClintock, and D. Garcia [both MRC Laboratory of Molecular Biology] for comments on the manuscript. Research was supported by UK MRC Awards MC_U105178790 and MC_UP_A025_1011 (to S.L.B. and A.P.C., respectively), Boehringer Ingelheim Fonds (PhD Fellowship to H.T.H.), the Wellcome Trust New Investigator Award WT100387 (to A.P.C.), European Molecular Biology Organization Young Investigator Award (to A.P.C.), and the European Commission Marie Curie Intra European Fellowship (to M.A.S.).

1. Schiavo G, Greensmith L, Hafezparast M, Fisher EM (2013) Cytoplasmic dynein heavy chain: The servant of many masters. *Trends Neurosci* 36(11):641–651.
2. Poirier K, et al. (2013) Mutations in *TUBG1*, *DYNC1H1*, *KIF5C*, and *KIF2A* cause malformations of cortical development and microcephaly. *Nat Genet* 45(6):639–647.
3. Lipka J, Kuijpers M, Jaworski J, Hoogenraad CC (2013) Mutations in cytoplasmic dynein and its regulators cause malformations of cortical development and neurodegenerative diseases. *Biochem Soc Trans* 41(6):1605–1612.
4. Weedon MN, et al. (2011) Exome sequencing identifies a *DYNC1H1* mutation in a large pedigree with dominant axonal Charcot-Marie-Tooth disease. *Am J Hum Genet* 89(2):308–312.
5. Willemsen MH, et al. (2012) Mutations in *DYNC1H1* cause severe intellectual disability with neuronal migration defects. *J Med Genet* 49(3):179–183.
6. Tsurusaki Y, et al. (2012) A *DYNC1H1* mutation causes a dominant spinal muscular atrophy with lower extremity predominance. *Neurogenetics* 13(4):327–332.
7. Scoto M, et al. (2015) Novel mutations expand the clinical spectrum of *DYNC1H1*-associated spinal muscular atrophy. *Neurology* 84(7):668–679.
8. Harms MB, et al. (2012) Mutations in the tail domain of DYNC1H1 cause dominant spinal muscular atrophy. *Neurology* 78(22):1714–1720.
9. Vissers LE, et al. (2010) A de novo paradigm for mental retardation. *Nat Genet* 42(12): 1109–1112.
10. Fiorillo C, et al. (2014) Novel dynein DYNC1H1 neck and motor domain mutations link distal spinal muscular atrophy and abnormal cortical development. *Hum Mutat* 35(3):298–302.
11. Strickland AV, et al. (2015) Mutation screen reveals novel variants and expands the phenotypes associated with *DYNC1H1*. *J Neurol* 262(9):2124–2134.
12. Gelineau-Morel R, et al. (2016) Congenital cataracts and gut dysmotility in a *DYNC1H1* dyneinopathy patient. *Genes (Basel)* 7(10):E85.
13. Niu Q, Wang X, Shi M, Jin Q (2015) A novel *DYNC1H1* mutation causing spinal muscular atrophy with lower extremity predominance. *Neurol Genet* 1(2):e20.
14. Allan VJ (2011) Cytoplasmic dynein. *Biochem Soc Trans* 39(5):1169–1178.
15. Carter AP (2013) Crystal clear insights into how the dynein motor moves. *J Cell Sci* 126(Pt 3):705–713.
16. Nicholas MP, et al. (2015) Control of cytoplasmic dynein force production and processivity by its C-terminal domain. *Nat Commun* 6:6206.
17. Hoogenraad CC, Akhmanova A (2016) Bicaudal D family of motor adaptors: Linking dynein motility to cargo binding. *Trends Cell Biol* 26(5):327–340.
18. Harms MB, et al. (2010) Dominant spinal muscular atrophy with lower extremity predominance: Linkage to 14q32. *Neurology* 75(6):539–546.
19. Harada A, et al. (1998) Golgi vesiculation and lysosome dispersion in cells lacking cytoplasmic dynein. *J Cell Biol* 141(1):51–59.
20. Eschbach J, et al. (2013) Dynein mutations associated with hereditary motor neuropathies impair mitochondrial morphology and function with age. *Neurobiol Dis* 58:220–230.
21. Garrett CA, et al. (2014) DYNC1H1 mutation alters transport kinetics and ERK1/2-cFos signalling in a mouse model of distal spinal muscular atrophy. *Brain* 137(Pt 7):1883–1893.
22. Ori-McKenney KM, Xu J, Gross SP, Vallee RB (2010) A cytoplasmic dynein tail mutation impairs motor processivity. *Nat Cell Biol* 12(12):1228–1234.
23. Sivagurunathan S, Schnittker RR, Nandini S, Plamann MD, King SJ (2012) A mouse neurodegenerative dynein heavy chain mutation alters dynein motility and localization in *Neurospora crassa*. *Cytoskeleton* 69(9):613–624.
24. Hafezparast M, et al. (2003) Mutations in dynein link motor neuron degeneration to defects in retrograde transport. *Science* 300(5620):808–812.
25. Schlager MA, Hoang HT, Urnavicius L, Bullock SL, Carter AP (2014) In vitro reconstitution of a highly processive recombinant human dynein complex. *EMBO J* 33(17):1855–1868.
26. Trokter M, Mücke N, Surrey T (2012) Reconstitution of the human cytoplasmic dynein complex. *Proc Natl Acad Sci USA* 109(51):20895–20900.
27. Miura M, Matsubara A, Kobayashi T, Edamatsu M, Toyoshima YY (2010) Nucleotide-dependent behavior of single molecules of cytoplasmic dynein on microtubules in vitro. *FEBS Lett* 584(11):2351–2355.
28. McKenney RJ, Huynh W, Tanenbaum ME, Bhabha G, Vale RD (2014) Activation of cytoplasmic dynein motility by dynactin-cargo adapter complexes. *Science* 345(6194):337–341.
29. Schroeder CM, Vale RD (2016) Assembly and activation of dynein-dynactin by the cargo adaptor protein Hook3. *J Cell Biol* 214(3):309–318.
30. Olenick MA, Tokito M, Boczkowska M, Dominguez R, Holzbaur EL (2016) Hook adaptors induce unidirectional processive motility by enhancing the dynein-dynactin interaction. *J Biol Chem* 291(35):18239–18251.
31. Belyy V, et al. (2016) The mammalian dynein-dynactin complex is a strong opponent to kinesin in a tug-of-war competition. *Nat Cell Biol* 18(9):1018–1024.
32. Jaarsma D, et al. (2014) A role for Bicaudal-D2 in radial cerebellar granule cell migration. *Nat Commun* 5:3411.
33. Baffet AD, Hu DJ, Vallee RB (2015) Cdk1 activates pre-mitotic nuclear envelope dynein recruitment and apical nuclear migration in neural stem sells. *Dev Cell* 33(6):703–716.
34. Hu DJ, et al. (2013) Dynein recruitment to nuclear pores activates apical nuclear migration and mitotic entry in brain progenitor cells. *Cell* 154(6):1300–1313.
35. Oates EC, et al.; UK10K (2013) Mutations in *BICD2* cause dominant congenital spinal muscular atrophy and hereditary spastic paraplegia. *Am J Hum Genet* 92(6):965–973.
36. Peeters K, et al. (2013) Molecular defects in the motor adaptor BICD2 cause proximal spinal muscular atrophy with autosomal-dominant inheritance. *Am J Hum Genet* 92(6):955–964.
37. Neveling K, et al. (2013) Mutations in *BICD2*, which encodes a golgin and important motor adaptor, cause congenital autosomal-dominant spinal muscular atrophy. *Am J Hum Genet* 92(6):946–954.
38. Ravenscroft G, et al. (2016) Recurrent de novo *BICD2* mutation associated with arthrogryposis multiplex congenita and bilateral perisylvian polymicrogyria. *Neuromuscul Disord* 26(11):744–748.
39. Fiorillo C, et al. (2016) Beyond spinal muscular atrophy with lower extremity dominance: Cerebellar hypoplasia associated with a novel mutation in *BICD2*. *Eur J Neurol* 23(4):e19–e21.
40. Splinter D, et al. (2010) Bicaudal D2, dynein, and kinesin-1 associate with nuclear pore complexes and regulate centrosome and nuclear positioning during mitotic entry. *PLoS Biol* 8(4):e1000350.
41. Matanis T, et al. (2002) Bicaudal-D regulates COPI-independent Golgi-ER transport by recruiting the dynein-dynactin motor complex. *Nat Cell Biol* 4(12):986–992.
42. Urnavicius L, et al. (2015) The structure of the dynactin complex and its interaction with dynein. *Science* 347(6229):1441–1446.
43. Deng W, et al. (2010) Neurodegenerative mutation in cytoplasmic dynein alters its organization and dynein-dynactin and dynein-kinesin interactions. *J Biol Chem* 285(51):39922–39934.
44. Paschal BM, Shpetner HS, Vallee RB (1987) MAP 1C is a microtubule-activated ATPase which translocates microtubules in vitro and has dynein-like properties. *J Cell Biol* 105(3):1273–1282.
45. Splinter D, et al. (2012) BICD2, dynactin, and LIS1 cooperate in regulating dynein recruitment to cellular structures. *Mol Biol Cell* 23(21):4226–4241.
46. Kon T, et al. (2012) The 2.8 Å crystal structure of the dynein motor domain. *Nature* 484(7394):345–350.
47. Schmidt H, Zalyte R, Urnavicius L, Carter AP (2015) Structure of human cytoplasmic dynein-2 primed for its power stroke. *Nature* 518(7539):435–438.
48. Redwine WB, et al. (2012) Structural basis for microtubule binding and release by dynein. *Science* 337(6101):1532–1536.
49. Schmidt H, Carter AP (2016) Review: Structure and mechanism of the dynein motor ATPase. *Biopolymers* 105(8):557–567.
50. Qiu R, Zhang J, Xiang X (2013) Identification of a novel site in the tail of dynein heavy chain important for dynein function in vivo. *J Biol Chem* 288(4):2271–2280.
51. MacArthur DG, et al. (2014) Guidelines for investigating causality of sequence variants in human disease. *Nature* 508(7497):469–476.
52. Mische S, et al. (2008) Dynein light intermediate chain: An essential subunit that contributes to spindle checkpoint inactivation. *Mol Biol Cell* 19(11):4918–4929.
53. Douglas PM, Dillin A (2010) Protein homeostasis and aging in neurodegeneration. *J Cell Biol* 190(5):719–729.
54. Antoniadi T, et al. (2015) Application of targeted multi-gene panel testing for the diagnosis of inherited peripheral neuropathy provides a high diagnostic yield with unexpected phenotype-genotype variability. *BMC Med Genet* 16:84.
55. Yu I, Garnham CP, Roll-Mecak A (2015) Writing and reading the tubulin code. *J Biol Chem* 290(28):17163–17172.
56. McKenney RJ, Huynh W, Vale RD, Sirajuddin M (2016) Tyrosination of α-tubulin controls the initiation of processive dynein-dynactin motility. *EMBO J* 35(11):1175–1185.